Experiments in Fluids 34 (2003) 285–290
DOI 10.1007/s00348-002-0558-9

An approximate amplitude attenuation correction for hot-film shear stress sensors

G.J. Kunkel, I. Marusic

Abstract A correction method, based on experimental results, has been developed to remedy the amplitude attenuation that occurs when statically calibrated hot-film shear stress sensors are used in air. The correction method is necessary in applications where typically two-dimensional arrays of measurement points are needed and other sensors, such as hot wires, cannot be employed. The method was developed with a primary aim of obtaining the correct power spectral density of an ensemble-averaged signature from an array of hot-film shear stress sensors. The hot-film sensors are corrected by comparing their individual power spectral densities to a reference spectrum obtained with a single hot wire, slightly elevated but within the viscous sublayer of the turbulent boundary layer. The method is verified by comparing the corrected hot film's turbulence statistics, power spectral density, and correlation coefficients with the corresponding results from the hot wire.

1 Introduction

Wall shear stress, or skin friction, is of fundamental importance in the characterization of any boundary layer. Instantaneous wall shear stress measurements are widely used in studies ranging from the analysis of large-scale structures in the turbulent boundary layer [21,5] to the testing of models of boundary conditions used in large-eddy simulations [19]. In all instances the correct characterization of the wall shear stress, mean and instantaneous, is crucial to the validity of such studies.

Of the several methods available for the time series measurement of wall shear stress (see [6] for a review), the hot-film sensor is perhaps the most commonly used. The problems associated with hot films used in air, mounted in the wall substrate, and calibrated statically have been studied previously by Alfredsson et al. [1] Bellhouse and Schultz [3] and Chew et al. [8], among others. These studies have found that while the mean wall shear stress can accurately be measured using hot-film probes in this manner, the energy content of the fluctuating wall shear stress cannot.

In a static calibration, the heat loss from the hot film to the wall substrate, while being unaffected by rapid fluctuations of the flow, is different for each calibration point due to the change in cooling of the substrate by the flow. Since the static calibration does not account for this change in heat loss, the amplitude of the instantaneous wall shear stress is underestimated. The greater the amount of heat transfer to the fluid through the substrate, the greater the underestimation of the instantaneous wall shear stress. For this reason, hot-film shear stress sensors perform better in fluids with relatively high thermal conductivity, such as oil and water, than in air. While Chew et al. [8] studied the limit of the dynamic response due to both amplitude attenuation and the inability of the hot film to follow an imposed frequency fluctuation, it was consistently the attenuation of the amplitude that was the limiting factor of the dynamic frequency response of the probes. Bellhouse and Schultz [3] and Ljus et al. [18] suggested that a dynamic calibration is necessary to correctly measure the fluctuating wall shear stress, while Chew et al. [8] and Alfredsson et al. [1] suggested a more accurate method of determining instantaneous wall shear stress is through the use of a slightly elevated hot wire.

Our motivation for the present study comes from an investigation using an array of hot-film sensors. In [19], an experiment was conducted to study a class of wall boundary conditions used in large-eddy simulations of turbulent boundary layers, which specify the instantaneous filtered wall shear stress based on the instantaneous filtered velocity at the first grid point above the wall. The boundary condition models were tested by comparing power spectral densities and correlation coefficients of the modeled filtered wall shear stress with the corresponding results of the actual measured filtered wall shear stress. To obtain the actual filtered wall shear stress, nine hot-film shear stress sensors were used. In a setup such as that used in [19] (shown in Fig. 1), it is impractical to build a dynamic calibration unit because of the complicated shaker rig required. It is also infeasible to use an array of slightly elevated hot wires because of the downstream disturbances the hot wires would cause. Therefore, a correction method was developed so that the amplitude attenuation of the hot film is remedied by forcing each of the individual hot films to have the correct power spectral density. The method is

Received: 9 October 2001 / Accepted: 8 October 2002
Published online: 19 December 2002

G.J. Kunkel, I. Marusic (✉)
Department of Aerospace Engineering and Mechanics, University of Minnesota, Minneapolis, MN 55455, USA
E-mail: marusic@aem.umn.edu

The authors gratefully acknowledge the financial support of the National Science Foundation through grants CTS-9983933 and ACI-9982274.

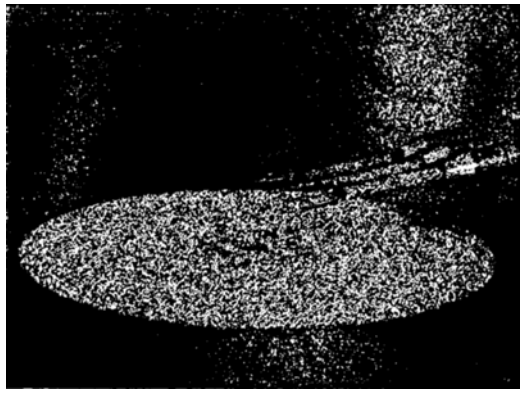

Fig. 1. Example experimental setup. (Source: [19]) Used with permission of Cambridge University Press

approximate in the sense that only the amplitude of the signature is being corrected and any time lag (shift in phase angle) between the measured and actual fluctuating wall shear stress is neglected.

The reference shear stress power spectral density was measured using a slightly elevated hot wire, which Khoo et al. [13] and Chew et al. [8] suggested gives a much more accurate representation of the energy content of the instantaneous wall shear stress. The amplitude of each frequency component of each of the Fourier series of the individual hot-film probe signatures was adjusted to give the correct amplitude found from the elevated hot wire. The correction function was determined using one representative hot-film probe and was applied to all hot-film probes used in the experiment. This was possible since the attenuations, as a function of frequency, were checked and found to be essentially the same for all of the hot films involved. It is important to note that although all of the hot-film probes were corrected using the correction function based on one representative hot film and one hot wire, all hot-film probes retained their original fluctuating characteristics. This work describes the correction method that was developed and verifies its results by comparison with other shear stress measurement studies.

A similar correction method is used in [18] to correct the power spectral density of the velocity of a hot-film wedge used in a two-phase flow. However, that method can only be used to correct the power spectral density. No consideration was given to correcting the instantaneous probe signatures and thus their correction was inapplicable to [19], where the individual signatures were needed to obtain the filtered wall shear stress. The correction in [18] was modeled after the theoretical and experimental study of Bellhouse and Schultz [2], which examined the dynamic sensitivities of hot-film probes used in air. Their correction function has a number of constants that must be determined by comparing the power spectral densities of the hot film and of a hot wire used at the same point in the flow. The constants are probe dependent, relying on probe geometry and material. The correction was tested by comparing spectra and turbulence intensities that were obtained through the integration of the spectra. No correlation coefficients, probability density functions, or higher order turbulence statistics were shown.

It is important to note that an ideal correction would need to account for both amplitude attenuation and any phase shifts across all frequencies. However, such a dynamic calibration would be extremely challenging, especially in applications with multiple sensors. There is also no conclusive evidence of the precise effects of any phase shifts on the measurement of wall shear stress. Cook [10] found that the hot-film sensors do exhibit some phase shift and Cook et al. [11] suggested that, for the type of sensors used in this study, it is approximately 12° over a frequency range of 3–20 Hz. Khoo et al. [14] and Moen and Schneider [20] used both electrical and velocity perturbation tests and found the maximum frequency response of such probes to be greater than 10 kHz, suggesting negligible lag at high frequencies. Similarly, Bellhouse and Schultz [3] suggested that the thermal feedback of the hot film does not occur at high frequencies due to the sharp attenuation of the thermal waves, again implying negligible phase shift at high frequencies. From these studies, it appears that there is a lag in hot-film shear stress signatures at low frequencies that does not exist at high frequencies. The frequency range over which this transition occurs is not known.

However, in this paper, we are primarily concerned with a correction method to obtain the correct filtered power spectral density from an array of hot-film shear stress sensors, such as that used in [19]. As described above, this involves ensemble averaging nine time series signatures to obtain a 'filtered' signature with its corresponding spectrum. Strictly, cross-correlations will exist between the nine signatures due to different individual sensor phase shifts, and thus will influence the final spectrum. However, it is expected that neglecting the phase shifts is a reasonable assumption. A simple test was used to help justify this assumption. Arbitrary phase shifts, over different frequency ranges, were applied to each of the individual hot-film shear stress signatures before filtering. The filtered spectra with the various phase shifts were then compared with the filtered spectrum obtained from the signatures without phase shifts. The tests showed the effect on the final filtered spectrum to be very minor, even with phase shift differences up to 75° between the sensor signals.

2 Experimental setup

All data were gathered in a nominally zero-pressure-gradient turbulent boundary layer 3.2 m downstream of a trip-wire where the boundary layer thickness δ was 64 mm. The Reynolds number based on momentum thickness $R_\theta = U_\infty \theta / \nu = 3{,}500$, where U_∞ is the free-stream velocity equal to 8.9 ms^{-1}, θ is the momentum thickness, and ν is the kinematic viscosity. The Reynolds number based on friction velocity $Re_\tau = U_\tau \delta / \nu = 1{,}350$, where the friction velocity $U_\tau = (-\langle \tau_w \rangle / \rho)^{\frac{1}{2}}$ and $\langle \tau_w \rangle$ is the mean (long-time-averaged) wall shear stress. The arrangement of the hot-film shear stress sensors used in [19] is shown in Fig. 1. Here, flow is from left to right and it is easy to see the flow blockage that would have occurred had elevated hot wires been used.

Of the nine TSI (Shoreview, Minn.) hot-film shear stress sensors used, eight were Model 1268, 1.5 mm diameter, and one was Model 1237, 3.2 mm diameter. The sensing elements on all of the hot films were of similar construction and were 0.15×1.5 mm (3×30 viscous wall units). The hot-film sensors were arranged in a 3×3 array with 6.02 mm between adjacent sensor centers and mounted in a 76-mm Delrin (DuPont, Wilmington, Del.) plug flush with the wind tunnel floor. The hot wire used to obtain the correct spectrum was held in the viscous sublayer at a non-dimensional wall-normal position of $z^+=zU_\tau/\nu=3.6$ above a 'non-conducting' glass wall with a thermal conductivity with respect to air of approximately 32. The hot-wire filament was made of tungsten wire with a diameter $d=5$ μm. The ends of the wire were coated with copper, leaving a sensing length of $l=1$ mm. The length-to-diameter ratio of the sensing element of the wire was therefore $l/d=200$. Scaled with wall units, $d^+=0.1$ and $l^+=20$. The frequency response of the hot wire and hot films, obtained from a square-wave test [6], were approximately 25 kHz and 10 kHz, respectively. Both the hot films and hot wire were operated with an AA Labs (A. A. Lab-Systems, Ramat Gan, Israel) AN-1003 10-channel constant-temperature anemometer. The hot films were run at an overheat ratio of 1.5, while the hot-wire overheat ratio was 1.7. All signals were conditioned with a Tektronix (Beaverton, Ore.) VX4780 signal conditioner and a Tektronix VX4244 16-bit resolution digitizer was used to sample the signals at a rate of 10 kHz for 105 s.

In [7], [9] and [16], the ratio of the sensing length to the diameter of the hot wire (l/d), the overheat ratio, and the conductivity of the wall substrate were found to have a significant effect on near-wall hot-wire measurements due to additional heat loss to the prongs and the wall. Therefore, the parameters of the hot wire, wall substrate, and wall height were chosen so as to keep these errors minimal. Figures 11 and 12 in [7] show that for a 'non-conducting' wall substrate, a hot wire positioned at $z^+=3.6$, with an $l/d=200$ and an overheat ratio of 1.7, there is negligible error expected in the measured mean velocity. Also, Krishnamoorthy et al. [16] found that there is no influence of the overheat ratio on the root mean square, skewness, and flatness of the velocity signature, and that the hot-wire diameter only effects these statistics for $z^+<3$.

Inadequate probe resolution can also significantly affect near-wall hot-wire measurements. The length of the sensing element determines the length over which the measurement is averaged in the spanwise direction. If this length is too large, the spanwise spatial averaging can cause an attenuation of the root mean square of the velocity signature and can also lead to inaccurate measurements of the skewness and flatness. This effect becomes more predominant as the wall is approached. Ligrani and Bradshaw [17] conclude that for $8<z^+<17.5$, the measured turbulence intensity is accurate within 4% for $l^+<20$–25, while the skewness and flatness are accurate within experimental error. These results are consistent with Khoo et al. [12], who show (see their Figs. 2–4) that a hot wire with similar characteristics as the one used in this study ($l^+=20$), fixed at $z^+=3.6$, yields a 3% error in the root-mean-square velocity fluctuation with respect to the friction velocity and a 10% and 4% error in the skewness and flatness factors, respectively. We regard these accuracies as acceptable for the purposes of the present study.

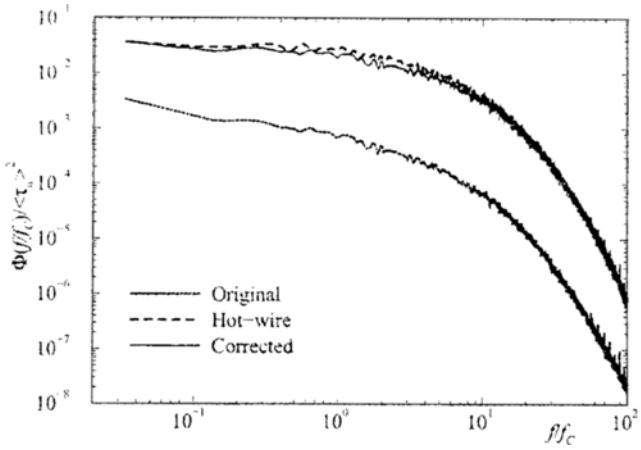

Fig. 2. Hot-film and hot-wire power spectral densities

The hot-film shear stress sensors were statically calibrated in situ against a Preston tube and the hot wire was calibrated in a separate calibration facility against a Pitot-static probe. The Delrin plug, in which the hot films were mounted, was allowed to reach thermal equilibrium at each calibration point. For both the hot films and the hot wire, fourth-order polynomial curves were used and in the case of the hot-films, as suggested by [4], higher order moment corrections were calculated and found to be negligible. The fluid temperature was monitored during the calibration and experiments and did not fluctuate by more than ±0.5°C.

3
Correction method and discussion

The correction method is applied to each of the individual probes. A summary of the procedure for the correction method is as follows:

1. Obtain the power spectral density of the hot film and the 'correct' power spectral density (in this instance, from the elevated hot wire).
2. Calculate the correction function, which is based on the positive square root of the ratio of the correct power spectral density (hot wire) to the power spectral density of the hot film.
3. Take the Fourier transform of the hot film, multiply by the correction function, and apply the inverse Fourier transform to obtain the corrected hot-film signature. These steps are detailed below.

3.1
Power spectral densities

The power spectral densities of the wall shear stress are defined as

$$\Phi(f) = \lim_{T\to\infty} \frac{1}{T}\{F.T.^*[\tau'(t)]F.T.[\tau'(t)]\} \ .$$

where ′ denotes a fluctuating quantity, f is frequency, F.T. denotes the Fourier transform and * denotes a complex conjugate. All spectra are normalized such that

$$\int_0^\infty \Phi(f)\mathrm{d}f = \left\langle \tau'^2 \right\rangle ,$$

where ⟨⟩ signify a long time average. The power spectral densities of the hot-film shear stress sensor before correction (original) and of the slightly elevated hot wire are shown in Fig. 2. It is easy to see the amplitude attenuation that occurs. Note that $\Phi(f/f_C)$ is defined as the power spectral density per non-dimensional frequency f/f_C, where $f_C=U_C/(2\pi\delta)$ is taken to be a constant, which is non-dimensionalized using the square of the mean wall shear stress ($\langle\tau_w\rangle^2$). Here, U_C, the convection velocity, is taken to be $0.82U_\infty$ following Uddin et al. [22], who concluded that a fixed convective speed was a reasonable assumption based on a survey of previous studies and from two-point double-velocity correlation measurements.

3.2 Ratio of the power spectral densities and correction function

The ratio of the power spectral densities and the curve fit of this ratio are shown in Fig. 3. The hot-wire and hot-film data sets consist of 1,048,576 points. To retain the set size, as well as capture the low frequencies, the ratio must be determined using the largest number of points possible. However, this leads to relatively large scatter in the spectra because of the small number of records over which the ensemble average is being taken. To resolve this, fewer samples are used, allowing for more realizations in the ensemble, which smooths the final spectra and thus the ratio. The ratio as a function of frequency is not exactly a constant as suggested in [1] and this is what prevents the signature from being corrected using a simple ratio of root mean squares. Various methods can be employed for determining the ratio function and here it was determined using error functions to blend characteristic lines.

The correction function is based on a curve fit of the following form:

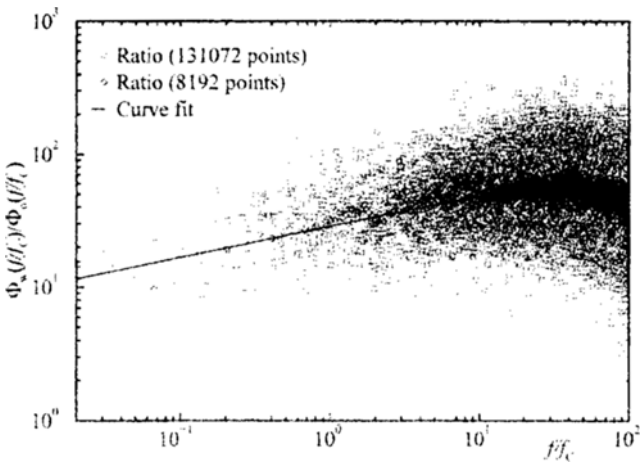

Fig. 3. Ratio of hot-wire to hot-film spectra

$$C(f) = \begin{cases} [\Phi_w(f)/\Phi_0(f)]^{\frac{1}{2}} & 0 < f \le f_s/2 \\ [\Phi_w(f_s-f)/\Phi_0(f_s-f)]^{\frac{1}{2}} & f_2/2 < f < f_s \end{cases}$$

The o and w subscripts denote the original hot-film and hot-wire terms, respectively. The zero-frequency component of the original hot film is not corrected since it contains the mean of the hot-film signature, which is assumed to be correct ($C(0)=1$). It is necessary to take the square root of the ratio function because the power spectral density is the product of the Fourier transform and its complex conjugate. Since the power spectral densities of both the hot wire and hot film are positive, the root is always defined and real. Notice that the desired end result of the correction (the hot-film shear stress signature having the correct power spectral density) is directly related to how well the ratio curve fit function describes the actual ratio of the power spectral densities. We expect that the correction function is dependent on Reynolds number and therefore must be recalculated for each flow independently. This is similar to Ljus et al. [18], who also found their correction function to depend on the Reynolds number.

3.3 Correction and discussion

Once the correction function is obtained, the amplitude attenuation of the hot-film signature can be rectified. First, the hot-film signature is transformed to the frequency domain using the Fourier transform:

$$F.T.[\tau_0(t)] = R_0(f) + I_0(f)j ,$$

where $R_o(f)$ and $I_o(f)$ are the real and imaginary parts of the Fourier transform of the original hot-film signature and $j=\sqrt{-1}$. Then, the coefficients (real and imaginary) at each frequency are multiplied by the correction function evaluated at the corresponding frequency:

$$R_c(f) = R_0(f)C(f) ,$$
$$I_c(f) = I_0(f)C(f) .$$

Finally, the hot-film shear stress signature is transformed back to the temporal domain using the inverse Fourier transform:

$$\tau_c(t) = F.T.^{-1}[R_c(f) + I_c(f)j] .$$

As discussed in Sect. 3.2, the size of the Fourier transforms will determine the final length of the hot-film signature. The phase angle of the Fourier transform of the original hot-film signature, $\tan^{-1}[I_o(f)/R_o(f)]$, is not affected by the correction function since both the real and the imaginary parts are multiplied by the same function.

The corrected hot-film power spectral density, along with original and hot-wire power spectral densities, are shown in Fig. 2. As expected, the agreement between the power spectral density from the hot wire and that of the corrected shear stress signature is very good. Representative wall shear stress signatures from the hot film before and after the correction are shown in Fig. 4. Qualitatively, the signatures show that although the hot film has been corrected to have the same energy content as the hot wire,

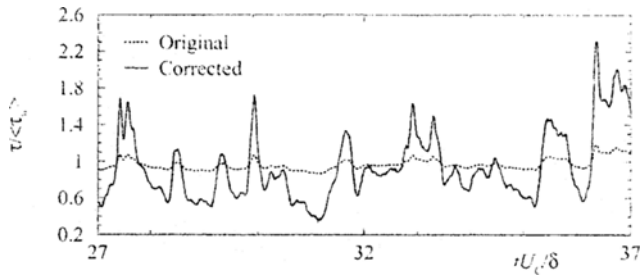

Fig. 4. Representative hot-film shear stress signatures

the individual fluctuating characteristics of the hot film remain. The relative root mean square with respect to the mean, the skewness, and the flatness of the shear stress measured from the hot film before and after correction, from the hot wire and those found in comparable experiments are shown in Table 1. The corrected hot-film shear stress sensor statistics agree well with the results of Alfredsson et al. [1], Chew et al. [8], and Kim et al. [15]. The simulation results of the latter [15] were obtained from the slope of the velocity profile in the viscous sublayer. The probability density functions corresponding to these statistics are shown in Fig. 5. The probability density function of the corrected sensor is seen to improve as it closer approaches the assumed correct probability density function of the hot wire. This is consistent with the improved skewness and flatness statistics shown in Table 1.

Correlation coefficients,

$$R_{\tau_a\tau_b}(T) = \frac{\langle \tau_a'(t)\tau_b'(t-T)\rangle}{\left(\langle \tau_a'^2\rangle\langle \tau_b'^2\rangle\right)^{1/2}},$$

are shown in Fig. 6. Here, T is the time delay between the two signatures, which are both non-dimensionalized by their root mean square values. Figure 6a shows the autocorrelation of the original and corrected hot-film signatures

Table 1. Turbulence statistics

	$\langle \tau'^2\rangle^{1/2}/\langle\tau\rangle$	Skewness	Flatness
Original	0.06	0.7	3.8
Hot wire	0.34	1.1	4.3
Corrected	0.36	0.9	4.4
Alfredsson et al. [1]	0.40	1.0	4.8
Chew et al. [8]	0.39	1.0	4.8
Kim et al. [15]	0.36	0.9	4.1

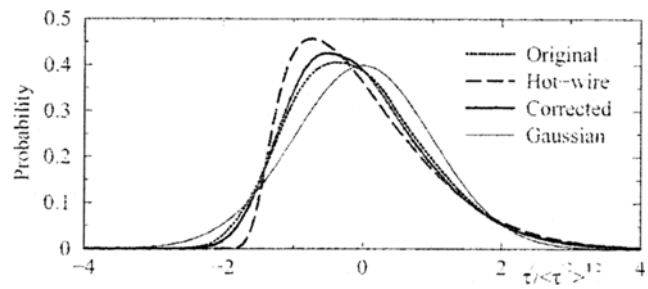

Fig. 5. Hot-film and hot-wire probability density functions

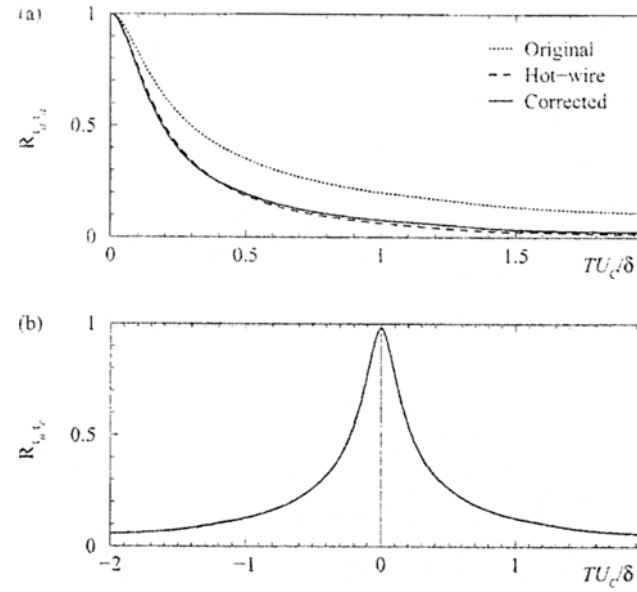

Fig. 6a, b. Hot-film and hot-wire autocorrelations and original and corrected hot-film cross-correlation

along with the autocorrelation of the hot-wire signature, while Fig. 6b shows the cross-correlation between the original and corrected hot-film signatures. Similar to the probability density functions, the autocorrelation of the corrected hot film follows the assumed correct autocorrelation from the hot wire. From the strong peak in the cross-correlation we see that the correction method has little effect on the phase of the wall shear stress signature.

It is important to note that while the turbulence statistics discussed above are greatly improved, there is still some difference between the corrected sensor's values and those suggested by other authors (Table 1). This difference is largely due to the method used to obtain the 'correct' power spectral density. In the other studies, more accurate methods were used to obtain the fluctuating wall shear stress, including but not limited to a hot wire with a smaller sensing element, a pulsed hot-wire, and laser Doppler velocimetry. Thus, the most significant limitation of the proposed correction method is the attainment of the correct power spectral density of the wall shear stress.

4
Summary and conclusions

It has long been known that the use of statically calibrated hot-film shear stress sensors in air, mounted in or on a wall substrate, is plagued with difficulties, resulting in the inaccurate measurement of the amplitude of the instantaneous wall shear stress. The use of a slightly elevated hot wire in the viscous sublayer of the boundary layer has been shown to better characterize the instantaneous wall shear stress. However, this is infeasible in multiple-probe arrangements where the probes are placed in an array in the stream-wise direction, resulting in flow disturbance and probe blockage. To overcome this obstacle and others, a correction method has been developed, which allows the use of a static calibration and greatly improves the measurement of the instantaneous wall shear stress. The correction method has been developed for applications

where the primary concern is a measure of the power spectral density of an ensemble-averaged signature from an array of hot-film shear stress sensors. The correction scheme involves matching the turbulent energy (amplitude) of the hot-film probe to that of a slightly elevated hot wire, which is assumed to give the correct reading. To obtain the corrected amplitude, the Fourier transform of the hot film is simply multiplied by the square root of the ratio of hot-film to hot-wire ensemble-averaged power spectral densities. The inverse Fourier transform is then applied to return the hot-film signature back to the time domain. The correction is shown to work well. The root mean square with respect to the mean, the skewness, and the flatness of the corrected hot-film shear stress signature equals 0.36, 0.9, and 4.1, respectively. These agree reasonably well with the results of previous experimental and computational studies.

References

1. Alfredsson PH, Johansson AV, Haritonidis JH, Eckelmann H (1988) The fluctuating wall-shear stress and the velocity field in the viscous sublayer. Phys Fluids 31:1026–1033
2. Bellhouse BJ, Schultz DL (1967) The determination of fluctuating velocity in air with heated thin-film gauges. J Fluid Mech 29:289–295
3. Bellhouse BJ, Schultz DL (1968) The measurement of fluctuating skin friction in air with heated thin-film gauges. J Fluid Mech 32:675–680
4. Breuer KS (1995) Stochastic calibration of sensors in turbulent flow fields. Exp Fluids 19:138–141
5. Brown GL, Thomas ASW (1977) Large structure in a turbulent boundary layer. Phys Fluids 20:S243–S252
6. Bruun HH (1995) Hot-wire anemometry. Oxford University Press, Oxford
7. Chew YT, Khoo BC, Li GL (1998) An investigation of wall effects on hot-wire measurements using a bent sublayer probe. Meas Sci Technol 9:67–85
8. Chew YT, Khoo BC, Lim CP, Teo CJ (1998) Dynamic response of a hot-wire anemometer. Part II: a flush-mounted hot-wire and hot-film probes for wall shear stress measurements. Meas Sci Technol 9:764–778
9. Chew YT, Shi SX, Khoo BC (1995) On the numerical near-wall corrections of single hot-wire measurements. Int J Heat Fluid Flow 16:471–476
10. Cook WJ (1994) Response of hot-element wall shear stress gages in unsteady turbulent flows. AIAA J 32:1464–1471
11. Cook WJ, Giddings TA, Murphy JD (1988) Response of hot-element wall shear stress gages in laminar oscillating flows. AIAA 26:706–713
12. Khoo BC, Chew YT, Li GL (1997) Effects of imperfect spatial resolution on turbulence measurements in the very near-wall viscous sublayer region. Exp Fluids 22:327–335
13. Khoo BC, Chew YT, Lim CP, Teo CJ (1998) Dynamic response of a hot-wire anemometer. Part I: a marginally elevated hot-wire probe for near-wall velocity measurements. Meas Sci Technol 9:751–763
14. Khoo BC, Chew YT, Teo CJ, Lim CP (1999) The dynamic response of a hot-wire anemometer: III. voltage perturbation versus velocity perturbation testing for near-wall hot-wire/film probes. Meas Sci Technol 10:152–169
15. Kim J, Moin P, Moser R (1987) Turbulence statistics in fully developed channel flow at low Reynolds number. J Fluid Mech 177:133–166
16. Krishnamoorthy LV, Wood DH, Antonia RA, Chambers AJ (1985) Effect of wire diameter and overheat ratio near a conducting wall. Exp Fluids 3:121–127
17. Ligrani PM, Bradshaw P (1987) Spatial resolution and measurement of turbulence in the viscous sublayer using subminiature hot-wire probes. Exp Fluids 5:407–417
18. Ljus C, Johansson B, Almstedt A-E (2000) Frequency response correction of hot-film measurements in a turbulent airflow. Exp Fluids 29:36–41
19. Marusic I, Kunkel GJ, Porté-Agel F (2001) Experimental study of wall boundary conditions for large-eddy simulation. J Fluid Mech 446:309–320
20. Moen MJ, Schneider SP (1994) The effect of sensor size on the performance of flush-mounted hot-film sensors. J Fluids Eng 116:273–277
21. Rajagopalan S, Antonia RA (1979) Some properties of the large structure in a fully developed turbulent duct flow. Phys Fluids 22:614–622
22. Uddin AKM, Perry AE, Marusic I (1997) On the validity of Taylor's hypothesis in wall turbulence. J Mech Eng Res Dev 19/20: 57–66